Large Band Simulation of the Wind Speed for Real Time Wind Turbine Simulators

Cristian Nichita, Dragos Luca, Brayima Dakyo, and Emil Ceanga

***Abstract*—In this paper we propose two modeling procedures for wind speed simulation. These procedures could be implemented on the structure of a wind turbine simulator during studies concerning stand-alone or hybrid wind systems. The evolution of a horizontal wind speed has been synthesized taking into account two components. The medium- and long-term component is described by a power spectrum associated to a specific site. The turbulence component is assumed to be dependent on the medium- and long-term wind speed evolution. It is considered as a nonstationary process. Two simulation methods for this component, using rational and nonrational filters are proposed. In both procedures, the turbulence model is defined by two parameters, which are either obtained experimentally, or adopted *a priori*, according to information from the considered site. Numerical results and implementation aspects are also discussed.**

***Index Terms*—Non-stationary signals, numerical simulation, power spectral density, real time systems, shaping filters, simulators, turbulence, wind speed, windmills.**

I. Introduction

THE investigation of wind power systems involves high performance wind turbine simulators, especially in the case of the development of optimal control solutions. Nowadays these systems have become necessary tools for research laboratories in this field. Real-time wind turbine simulators are based on "wind powered like shafts", providing the static and dynamic characteristics for a given wind turbine [1]–[5].

A brief review of the literature points out different categories of real-time wind turbine simulators, depending on their design approach.

The most usual simulator structure is based on the DC motor current control [1], [2], [6], [7]. This current is the electrical image of the torque developed by the wind turbine on its shaft.

Other types of simulators are those with a general structure, using any type of servomotor [3], [5]. The architecture of such simulators is presented in Fig. 1. This simulator includes two sub-systems:

1) a real time software simulator (RTSS), which implements the mathematical model of the wind turbine and contains the wind speed generator (WG);
2) an electromechanical tracking system (ETS), which receives the set point from the RTSS (shaft speed/torque reference) and provides an output variable (torque/shaft speed), transmitted by the transducer Tr as a response variable to the RTSS.

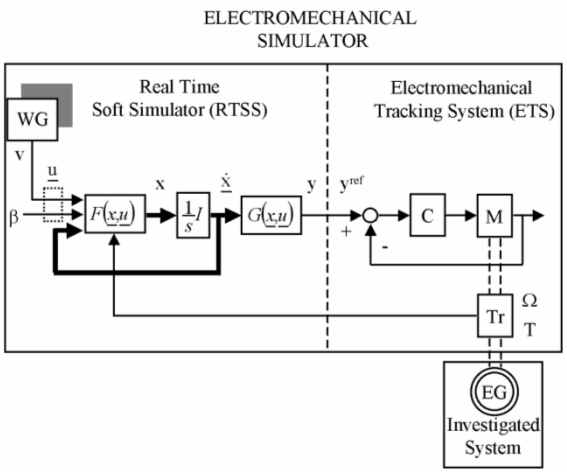

Fig. 1. Simulator with a general structure using any type of servomotor.

The RTSS is based on the dynamic wind turbine model. Generally, such a model can be described by a set of differential equations

$$\dot{\underline{x}}(t) = \underline{F}\left(\underline{x}(t), \underline{u}(t), t\right) \tag{1}$$

$$y(t) = G\left(\underline{x}(t), t\right) \tag{2}$$

where u and x are the input and state variables, respectively and F and G are nonlinear functions.

The vector describing the input data, u, includes the wind speed $v(t)$ and the pitch blade angle β (variable pitch case). The output variable y of the RTSS characterizes the dynamical behavior of the simulator shaft and represents the reference signal, y^{ref}, for the ETS.

Wind speed modeling is important, because the performances of the WG determine the features offered by the simulator for:

1) prediction of the energy output [8], [9];
2) analysis of the energy conversion and system dynamics [10]–[12];
3) development of Wind/Diesel systems control strategies [13], [14].

This paper deals with the design of a digital wind speed generator (WG) that can be included in the structure of the RTSS, given in Fig. 1. This sub-system reproduces short-, medium- and long-term wind speed fluctuations. The basic results used from the literature are:

1) Van der Hoven's model, considered in [15] and [16] as a one of the best known references in large-band wind speed modeling;

Manuscript received February 12, 2001; revised January 15, 2002. The authors would like to thank the NORELEC Company for their financial and technical support.

C. Nichita, D. Luca and B. Dakyo are with the GREAH, Université du Havre, 76600 Le Havre, France.

E. Ceanga is with the University "Dunarea de Jos", Galati, Romania.

Digital Object Identifier 10.1109/TEC.2002.805216

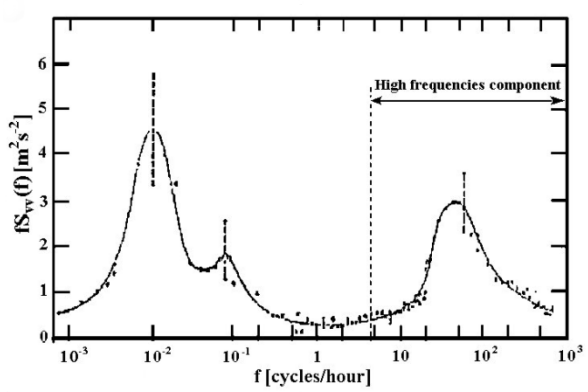

Fig. 2. Van der Hoven's spectral model.

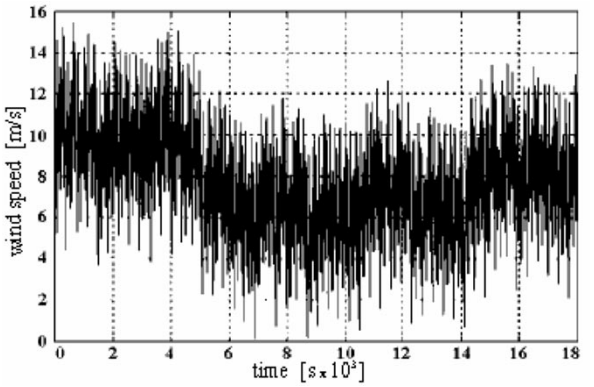

Fig. 3. Van der Hoven's model based simulation of the wind speed for a time horizon of 5 h.

2) von Karman's model for the short-term component [11], [16], [17].

We developed a mathematical model that describes both the turbulence (the short-term component) and the medium-term and long-term wind speed evolution (slower components).

In the following Section II, two wind speed models are analyzed, namely Van der Hoven's model [18] and von Karman model, used in [17]. Based on this analysis, Section III proposes two procedures for the generation of the wind speed as a nonstationary random process. Both procedures use two parameters that characterize the considered site. Section IV presents the numerical results obtained with the proposed procedures. Finally, some concluding remarks are given in Section V.

II. Large-Band Modeling of Wind Speed

In hybrid wind-diesel systems studies, the Van der Hoven model (Fig. 2) is considered as a reference model for the wind speed [15].

The power spectrum of the horizontal wind speed is calculated in a range from 0.0007 to 900 cycles/h, i.e., more than six decades. Such a frequency range contains the spectral domain that describes the medium and long-term variations, as well as the spectral range of the turbulence component.

Starting from Van der Hoven's model, we have developed a numerical wind speed simulation procedure, based on sampling the spectrum.

Let us consider ω_I, $i = \overline{1, N+1}$, the discrete angular frequency and $S_{vv}(\omega_i)$ the corresponding values of the power spectral density. The harmonic at frequency ω_i has an amplitude A_i

$$A_i = \frac{2}{\pi}\sqrt{\frac{1}{2}\left[S_{vv}\left(\omega_i\right) + S_{vv}\left(\omega_{i+1}\right)\right] \cdot \left[\omega_{i+1} - \omega_i\right]} \quad (3)$$

and a phase, φ_i, which is randomly generated, with an uniform distribution in the domain $[\pi, -\pi]$ [19], [20].

The wind speed, $v(t)$, is simulated with the relation

$$v(t) = \sum_{i=0}^{N} A_i \cos\left(\omega_i t + \varphi_i\right) \quad (4)$$

with $\omega_0 = 0$, $\varphi_0 = 0$ and $A_0 = \bar{v}$, where $\bar{v}$ is the mean wind speed, calculated on a time horizon greater than the largest period in Van der Hoven's characteristic (i.e., $T = 2\pi/\omega_1$). We adopted $N = 55$ for the sampling operation of the Van der Hoven characteristic and we considered the following discrete frequencies: $f_i = i \cdot 10^k$ [cycles/h], for $i = 1, 2,\ldots,9$ and $k = -3, -2, -1, 0, 1, 2$.

Fig. 3 presents fluctuations in wind speed over a 5-h period, simulated using (3) and (4).

One can notice that:

1) there are large variations in the mean wind speed, which gives proof of the capability of the Van der Hoven model to characterize wind behavior over the medium- and long-term;
2) the turbulence in Van der Hoven's model has the same magnitude regardless of the mean wind speed.

Consequently, the Van der Hoven model cannot be used for a complete description of the wind speed over a time scale of seconds, minutes, hours, because this model has a major drawback: the turbulence component is treated as a stationary random process. Its properties do not depend on the "mean" value variations, which are corresponding to the low frequencies domain and have a time scale of hours, days, etc.

The basic model of the turbulence component is given by the von Karman power spectrum [11]

$$S_{vv}(\omega) = \frac{0.475\sigma^2 \frac{L}{\bar{v}}}{\left[1 + \left(\frac{\omega L}{\bar{v}}\right)^2\right]^{5/6}} \quad (5)$$

where σ is the turbulence intensity and L is the turbulence length scale. This model shows that the turbulence component characteristic depends on the value of the mean speed $\bar{v}$.

In [17], the authors deal with a simulation scheme where the nonstationary turbulence component is modeled using a shaping filter with white noise input. The transfer function of the shaping filter is [11], [16], [17]

$$H_F(j\omega) = \frac{K_F}{\left(1 + j\omega T_F\right)^{5/6}} \quad (6)$$

where the static gain K_F is obtained from the condition that the variance of the resulting colored noise $w_c(t)$ is equal to 1. This condition is obtained with the following relation between parameters K_F and T_F

$$K_F \approx \sqrt{\frac{2\pi}{B\left(\frac{1}{2}, \frac{1}{3}\right)} \cdot \frac{T_F}{T_s}} \quad (7)$$

where T_s is the sampling period and B designates the beta function [17]. In order to obtain the turbulence component, $v_t(t)$, the colored noise $w_c(t)$ is multiplied by the estimated value of the standard deviation, $\hat{\sigma}_v$

$$v_t(t) = \hat{\sigma}_v \cdot w_c(t). \tag{8}$$

The two parameters: $\hat{\sigma}_v$ and T_F are calculated according to the mean value of the wind speed, $\bar{v}_m$

$$\hat{\sigma}_v = k_{\sigma,v} \cdot \bar{v}_m \tag{9}$$

$$T_F = \frac{L}{\bar{v}_m} \tag{10}$$

where: $k_{\sigma,v}$ is determined experimentally as the slope of the regression curve that statistically describes the relation between $\bar{v}_m$ and $\hat{\sigma}_v$. This wind speed generating model can be adapted to the specificities of a given site, by the use of the turbulence length scale L and the parameter $k_{\sigma,v}$ which characterize it. However, it does not allow the simulation of low frequency fluctuations over a period of minutes, hours, days and beyond.

III. Numerical Wind Speed Generator for Wind Turbine Simulator

The main purpose of our approach for a wind speed generator is to provide a simulation tool for the estimation of the wind resource and its variability. In different applications, the available nonstationary wind power is a quantity that is of interest.

For instance, when developing control strategies for hybrid wind/diesel systems, a description of the wind speed is necessary both in the short-term and the medium and long-terms. The turbulence model is used into the control law of the wind turbine, if we also use a performance criterion that takes into account simultaneously the efficiency of the conversion and the torque variations of the shaft (in order to reduce the fatigue implications [16]).

The control strategy of the system formed by wind turbine + diesel generator + batteries + flywheel concerns the operation of each component under full load, based on its specific wind speed evolution [14].

In a wind/diesel system experimental plant, the wind speed numerical generator should generate both turbulence and slower fluctuation components. For the short-term component, the wind model is similar to the wind speed when measured with an anemometer.

The solution proposed hereafter is based on the following remarks, highlighted in the previous section:

1) the method based exclusively on the Van der Hoven model leads to less accurate results, as the turbulence component is not modeled as a nonstationary process;
2) the procedure used in [17], based on the von Karman spectrum, allows the modeling of the turbulence component as a nonstationary process, but does not reproduce slow fluctuations, which correspond to the low frequency domain in the spectral characteristic of the wind speed.

Consequently, we thought that combining the low frequency model of Van der Hoven's characteristic with a nonstationary turbulence model would result in a new simulation method, described below, which is better adapted to the above mentioned demands.

We made the assumption that the discrete frequency values $f_0 = 0$, $f_1 = 0.001$ cycles/h, $\ldots$, $f_{30} = 3$ cycles/h Van der Hoven's model correspond to the spectral range that describes medium- and long-term wind speed evolution. The turbulence component (i.e., the short-term component) is given by the spectral range between 4 cycles/h and 1000 cycles/h. In this case, $v(t)$ becomes

$$v(t) = v_{ml}(t) + v_r(t) \tag{11}$$

where

1) $v_{ml}(t)$ is the medium- and long-term component, being calculated with (4), where $N = 30$,

$$v_{ml}(t) = \sum_{i=0}^{30} A_i \cos(\omega_i t + \varphi_i); \tag{12}$$

2) $v_t(t)$ is the turbulence component.

We have considered that Van der Hoven's model can only describe the wind variation correctly on a large time scale, so $v_{ml}(t)$ will be used in the final wind model. This solution must be used because the experimental identification of the spectral characteristic of the wind speed in the very low frequency range is difficult, as it requires records over a long period of time.

We adopted the Van der Hoven model as a result available for the temperate area, which offers a spectral description of the wind speed in the low frequency domain (0.0007 cycles/h…4 cycles/h).

For preliminary studies with wind turbine simulators, it is often enough to make use of general information concerning the site. The generation of short-term wind speed fluctuations is performed by using the turbulence length scale (L) and the slope of the regression curve, $k_{\sigma,v}$, both defined previously. These parameters are correlated: for the coast and offshore sites, the turbulence length scale is small (i.e., 100–200 m), as well as the slope $k_{\sigma,v}$ (i.e., 0.1…0.15). In cases where the influence of the site's topography is more important, the values of L and $k_{\sigma,v}$ are higher (i.e., 200…500 m and 0.15…0.25, respectively) [17].

Let us now consider that parameters L and $k_{\sigma,v}$ are found, either by experimental identification, or by adopting them according to the site's characteristics. We have used two time scales for the simulation of the wind speed. T_{s1} (minutes ranges) is the sampling period for the $v_{ml}(t)$ component, while T_s, (seconds ranges) was used to sample $v_t(t)$. Two solutions can be used in order to generate the nonstationary component $v_t(t)$.

A. Procedure 1

This procedure for the large-band wind simulation consists of the following steps.

1) Generate with (12) the current value of the medium- and long-term component, $v_{ml}(t)$, using the sampling period T_{s1}. Let i be the current step of the procedure and $v_{ml}(iT_{s1})$ the generated value of this component.
2) Update the parameters of the turbulence component model, at the beginning of the current interval $[iT_{s1}, (i+1)T_{s1}]$. We suppose that on a time scale of the

variable $v_t(t)$, the long -and medium-term component is considered as the mean value of the wind speed (noted $\overline{v}_m$ in the previous section). The current values of the parameters in the turbulence component model are:

$$T_F^{(i)} = \frac{L}{v_{ml}\,(iT_{s1})} \tag{13}$$

$$\hat{\sigma}_v^{(i)} = k_{\sigma,v} \cdot v_{ml}\,(iT_{s1}) \tag{14}$$

$$K_F^{(i)} \approx \sqrt{\frac{2\pi}{B\left(\frac{1}{2},\frac{1}{3}\right)} \cdot \frac{T_F^{(i)}}{T_s}}. \tag{15}$$

3) Calculate the discrete impulse response of the filter (5) with parameters $K_F^{(i)}$ and $T_F^{(i)}$, using the equation:

$$h^{(i)}(t) = \frac{2}{\pi}\int_0^{\infty} P^{(i)}(\omega)\cos(\omega t)d\omega \tag{16}$$

where

$$P^{(i)}(\omega) = Re\left[\frac{K_F^{(i)}}{\left(1+j\omega T_F^{(i)}\right)^{5/6}}\right]. \tag{17}$$

This response is calculated using the sampling period T_s and a finite limit in the integral (16).

4) Generate the turbulence component in the interval $[iT_{s1}, (i+1)T_{s1}]$, using the convolution

$$v_t^{(i)}(t) = \int_0^t h^{(i)}(\tau)w(t-\tau)d\tau \tag{18}$$

with sampling period T_s.

5) Calculate the current value of the wind speed

$$v(t) = v_{ml}\,(iT_{s1}) + \sigma_v^{(i)} \cdot v_t^{(i)}(t) \tag{19}$$

with sampling period T_s.

6) Do $i = i+1$ and return to step 1.

The variables $h^{(i)}(k) \equiv h^{(i)}(kT_s)$ and $v_t^{(i)}(m) \equiv v_t^{(i)}(mT_s)$ are calculated with:

$$h^{(i)}(k) = \frac{2}{\pi}T_s \cdot \Delta\omega \sum_{r=0}^{M} P^{(i)}(r)\cos\left(krT_s\Delta\omega\right) \quad k = \overline{0,N} \tag{20}$$

$$v_t^{(i)}(m) = T_s \cdot \sum_{p=0}^{N} h^{(i)}(p)w_c(m-p) \tag{21}$$

where

$$P^{(i)}(r) = Re\left[\frac{K_F^{(i)}}{\left(1+jr\Delta\omega \cdot T_F^{(i)}\right)^{5/6}}\right], \quad r = \overline{0,M} \tag{22}$$

and the parameters M and N are adopted so that

$$P(\omega)|_{\omega > M\cdot\Delta\omega} \cong 0; \quad h(t)|_{t > N\cdot T_s} \cong 0. \tag{23}$$

In order to limit the numerical errors, the parameters $\Delta\omega$, T_s, M and N are chosen so that the static gain of the nonparametric filter, $\hat{K}_F$, established according to the impulse response (20), *i.e.*

$$\hat{K}_F = T_s \cdot \sum_{k=0}^{N} h(k) \tag{24}$$

should correspond to the K_F parameter of (5).

Adopting $\Delta\omega = 0.002$ s^{-1}, $M = 5000$, $T_s = 1$ s and $N = 100$, the error is below 1% ($\hat{K}_F = 5.332$, given $K_F = 5.3$). This error will become more important when the step $\Delta\omega$ gets larger. For example, when step $\Delta\omega$ is doubled, the error reaches 7%. Figs. 4 and 5 show the curves of functions $P(\omega)$ and $h(t)$, respectively, with $K_F = 5.3$ and $T_F = 18$ s.

For an accurate conversion between the transfer function $H(j\omega)$ and the impulse response $h(k)$, a small step $\Delta\omega$ must be adopted. This conversion is made at each step i of the algorithm, so it requires considerable effort in calculation.

There are no difficulties to use the presented procedure for off-line applications (estimation of the generated power, etc.). For a wind turbine simulator, the most of the computing power must be allocated for the real time simulation of the turbine, because its model is complex [3]. The generation of the wind speed involves the transforming of the shaping filter in a finite impulse response (FIR) filter with N parameters, which provides the $v_t(t)$ component. These parameters are updated every T_{s1} period, by calculating the frequency characteristics $P(\omega)$ in M points. It is obvious that using this procedure in the real

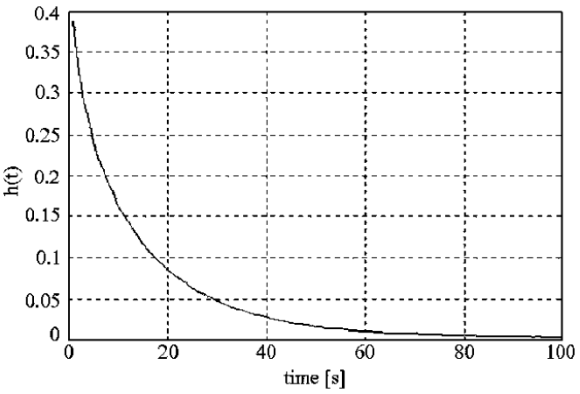

Fig. 4. Impulse response of the shaping filter (5).

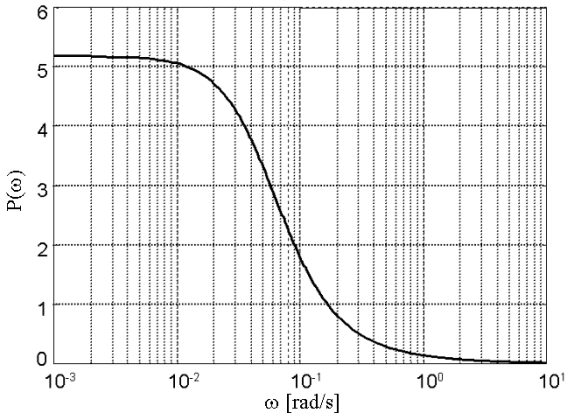

Fig. 5. $P(\omega)$ function of the shaping filter (5).

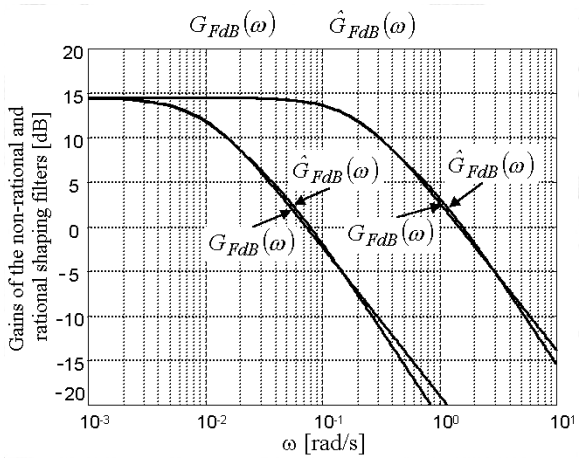

Fig. 6. Gain characteristics of the nonrational and rational shaping filters.

time software of the wind turbine simulator wouldn't be very appropriate, because the precision requirements of the numerical calculus impose high values for N and M (e.g., $N = 100$ and $M = 5000$).

B. Procedure 2

A simple solution to reduce the computational time is to approximate the 5/6-order filter by a rational transfer function. An acceptable solution for the model approximation is achieved with the transfer function

$$\hat{H}_F(s) = K_F \frac{(m_1 T_F s + 1)}{(T_F s + 1)(m_2 T_F s + 1)} \tag{25}$$

where $m_1 = 0.4$ and $m_2 = 0.25$. Fig. 6 shows the Bode characteristics $G_{F\mathrm{dB}}(\omega) = 20\log|H_F(j\omega)|$ and $\hat{G}_{F\mathrm{dB}}(\omega) = 20\log|\hat{H}_F(j\omega)|$. This comparison is made for two different values of the time constant T_F: 5 s and 100 s. We notice a very good approximation of the nonrational filter, in a large frequency range.

The generation of nonstationary wind speed with the rational filter (25) includes the following steps.

1) Calculate the medium- and long-term value of wind speed, $v_{ml}(iT_{s1})$, as in Procedure 1.
2) Calculate parameters $T_F^{(i)}$ and $\hat{\sigma}_v^{(i)}$ with (13) and (14).
3) Calculate the static gain of the filter, $K_F^{(i)}$, so that the colored noise at the filter output should have a normalized standard deviation ($\sigma_v^* = 1$). The input white noise of the filter, $w(t)$, is synthetically generated with sampling period T_s, having unitary variance ($\sigma_w^2 = 1$) and band-limited power spectral density

$$S_w(\omega) = S_{w0}, \quad \omega \in \left[-\frac{\omega_s}{2}, \frac{\omega_s}{2}\right] \tag{26}$$

Since S_{w0} satisfies to $\sigma_w^2 = 1/(2\pi)\int_{-\omega_s/2}^{\omega_s/2} S_{w0} d\omega = 1$, its value is $S_{w0} = T_s$. The variance of the colored noise at the filter output can be expressed as:

$$\begin{aligned} o_{v_t}^{2,(i)} &= \frac{1}{2\pi}\int_{-\omega_s/2}^{\omega_s/2} \left|\hat{H}_F^{(i)}(\omega)\right|^2 S_{w0} d\omega \\ &= \frac{T_s}{\pi}\int_{0}^{\omega_s/2} \left|\hat{H}_F^{(i)}(\omega)\right|^2 d\omega \end{aligned} \tag{27}$$

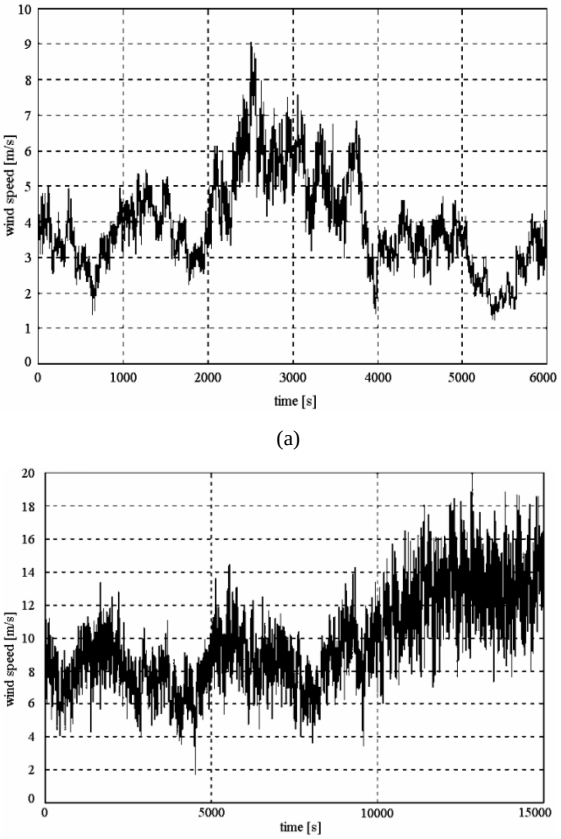

Fig. 7. Profiles of the generated nonstationary wind speed, using the adjustable shaping filter (5), for time horizons 6000 s (a) and 15 000 s (b). (a) time horizon of 6000 s. (b) time horizon of 15 000 s.

By imposing the condition $o_{v_t}^{2,(i)} = 1$, the static gain of the filter results in:

$$K_F^{(i)} = \sqrt{\frac{\pi}{T_s \Delta\omega \cdot S^{(i)}}} \tag{28}$$

where $\Delta\omega$ is the sampling step of the frequency and

$$S^{(i)} = \sum_{k=0}^{J} \frac{\left(m_1 T_F^{(i)} k\Delta\omega\right)^2 + 1}{\left[\left(T_F^{(i)} k\Delta\omega\right)^2 + 1\right] \cdot \left[\left(m_2 T_F^{(i)} k\Delta\omega\right)^2 + 1\right]} \tag{29}$$

with $J = \omega_s/(2 \cdot \Delta\omega)$.

4) Calculate the parameters of the sampled transfer function of the filter, $\hat{H}(z^{-1})$ and generate the turbulence component of the wind speed $v_t^{(i)}(t)$.
5) Calculate the wind speed using (19).

IV. Numerical Results

Fig. 7 presents two profiles of nonstationary wind speed, generated using the procedure 1, for time horizons of 6000 s and 15 000 s, respectively.

The chosen parameters in the algorithm were: $L = 180$ m, $k_{\sigma,v} = 0.16$, $T_{s1} = 180$ s., $T_s = 1$ s, $\Delta\omega = 0.002$ rad/s., $M = 5000$ and $N = 100$.

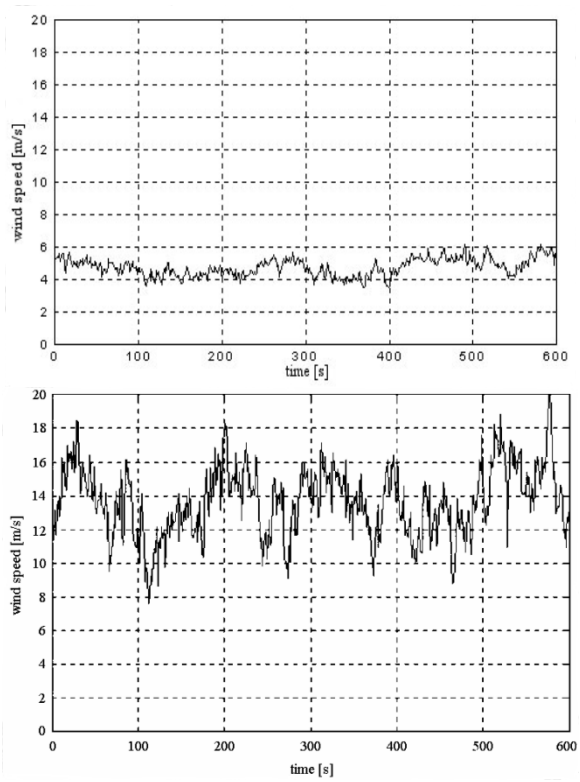

Fig. 8. Profiles for short-time horizon (600 s) of the generated wind speed, with different values of the mean speed: $v_{ml} = 5$ m/s (a); $v_{ml} = 13$ m/s (b).

In order to achieve a more detailed view of the turbulence component, Fig. 8 shows the evolution of the wind speed during two time intervals of 10 minutes each.

These intervals have been chosen so that the medium and long-term component, v_{ml}, has different values: 5 m/s and 13 m/s.

For the wind turbine simulator of the GREAH Laboratory (Le Havre University—France), the implementation of the algorithm based on the adjustable nonrational shaping filter (Procedure 1) is difficult, because of the long calculation time.

However, the procedure 2 reduces considerably this computational effort (more than ten times), thus making it more attractive for implementation in the RTSS of the wind turbine simulator. Fig. 9 presents a profile of wind speed, generated by means of this procedure for a time horizon of 5 h. Because the rational filter (25) approximates the nonrational filter (5) with a very small error (see Fig. 6), this procedure gives results close to those given by procedure 1.

The following remarks are necessary if we want to evaluate the numerical results.

1) The numerical procedures of simulation are based on a given model of the components $v_{ml}(t)$ and $v_t(t)$. If the values for the sampling parameters mentioned in Section III are respected, the numerical errors are within acceptable limits. So, the initial model can be reconstructed with the generated data.
2) The fundamental issue concerns the general method used as the basis of the two procedures. We have made the hypothesis that the nonstationary large band process can be approximated by a succession of stationary processes. Those are generated by a shaping filter having its parameters adjusted periodically according to the up-dated value of the medium- and long-term component. This component is treated as a stationary process (the first three decades of the Van der Hoven characteristics are involved).

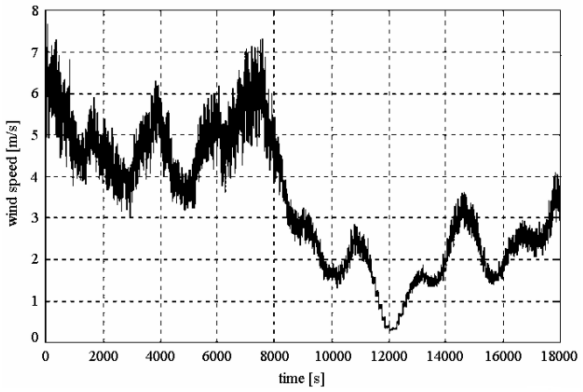

Fig. 9. Profile of the generated nonstationary wind speed, using the adjustable shaping filter (25), for a time horizon of 5 h.

Although this hypothesis somewhat simplifies reality, the samples obtained this way are similar to experimental records (see [17]).

If we compare the wind profiles in Figs. 7 and 9 with the one in Fig. 3, we can state that the solution proposed for the large band prediction of the wind speed is much more realistic than the one that results from the Van der Hoven model.

V. Conclusion

In order to improve the performances of real-time wind speed simulator, it is essential that the internal wind speed generator reproduce, as faithful as possible, the real conditions concerning the wind speed regime. The proposed wind speed generator considers the wind speed as a nonstationary process, having two components:

1) the long- and medium-term component, modeled by the low frequency range of an experimental available spectral characteristic (e.g., the Van der Hoven model in the range [0.0007 cycles/h–5 cycles/h]);
2) the turbulence component, described by a von Karman model with adjustable parameters, depending on the "mean" values.

Two procedures for nonstationary turbulence component generation, using adjustable shaping filters, are proposed in the paper. The first procedure, based on the noninteger order filter (5), leads to a nonparametric simulation model, requiring considerable computational effort. The second procedure, which uses the rational shaping filter (25), is much faster and therefore more attractive for implementation in the wind turbine simulator. In both cases, the turbulence model is defined by only two parameters, L and $k_{\sigma,v}$, whose values are either obtained experimentally, or adopted *a priori* according to the information regarding the considered site.

Finally, we would like to mention that the modeling procedures developed in our laboratory and presented in this paper

are currently under experimentation at a reference site, located near Fécamp, in Normandy, France.

REFERENCES

[1] W. M. Stein, J. F. Manwell, J. G. , and McGowan, "A power electronics based power shedding control for windwind/diesel systems," *Int. J. Ambient Energy*, vol. 13, no. 2, pp. 65–74, 1992.

[2] P. E. Battaiotto, R. J. Mantz, and P. F. Puleston, "A wind turbine emulator based on a dual DSP processor system," *Control Eng. Practice*, vol. 4, no. 9, pp. 1261–1266, 1996.

[3] C. Nichita, A. D. Diop, J. J. Belhache, B. Dakyo, and L. Protin, "Control structures analysis for a real time wind system simulator," *Wind Eng.*, vol. 22, no. 6, pp. 275–286, 1998.

[4] J. L. Rodriguez_Amenedo, F. Rodriguez-Garcia, J. C. Burgos, M. Chinchilla, S. Arnalte, and C. Veganzones, "Experimental ring to emulate wind turbines," in *Proc. ICEM Conf.*, vol. 3/3, Istanbul, Turkey, 1998, pp. 2033–2038.

[5] A. D. Diop, C. Nichita, J. J. Belhache, B. Dakyo, and E. Ceanga, "Modeling of a variable pitch HAWT characteristics for a real-time wind turbine simulator," *Wind Eng.*, vol. 23, no. 4, pp. 225–243, 1999.

[6] A. A. C. Nunes, P. C. Cortizo, and B. R. Menezes, "Wind turbine simulator using a DC machine and a power reversible converter," in *Proc. ICEMA Conf.*, Adelaide, Australia, 1993, pp. 536–540.

[7] F. Barrero, J. L. Mora, M. Perales, A. Marchante, E. Calvan, J. M. Carrasco, A. Torralba, and L. G. Franquelo, "A test-ring to evaluate a wind turbine generation control system based on DSP," in *Proc. EPE'97 Conf.*, Trondheim, Norway, 1997, pp. 2642–2645.

[8] C. S. Brune, R. Spee, and A. K. Wallace, "Experimental evaluation of a variable-speed double-fed wind-power generation system," *IEEE Trans. Ind. Applicat.*, vol. 30, pp. 648–655, May/June 1997.

[9] R. Pena, J. C. Clare, and G. M. Asher, "Doubly fed induction generator using back-to-back PWM converters and its application to variable-speed wind-energy generation," *Proc. Inst. Elect. Eng.*, vol. 143, no. 3, pp. 231–241, 1996.

[10] W. E. Leithead, "Dependence of performance of variable speed wind turbines on the turbulence," *Proc. Inst. Elect. Eng. C*, vol. 137, no. 6, pp. 403–413, 1990.

[11] W. E. Leithead, S. de la Salle, and D. Reardon, "Role and objectives of control for wind turbines," *Proc. Inst. Elect. Eng. C*, vol. 138, no. 2, pp. 135–148, 1991.

[12] B. Connor and W. E. Leithead, "Investigation of a fundamental trade-off in tracking the Cp max curve of a variable speed wind turbine," in *Proc. 12th BWEA Conf.*, Abingdon, U.K., 1993, pp. 313–319.

[13] W. Q. Jeffries, J. G. McGowan, and J. F. Manwell, "Development of a dynamic model for no storage wind/diesel system," *Wind Eng.*, vol. 20, no. 1, pp. 27–39, 1996.

[14] P. S. Panickar, S. M. Islam, and C. V. Nayar, "A new quasioptimal algorithm for a wind-diesel hybrid system," *Wind Eng.*, vol. 22, no. 3, pp. 159–169, 1998.

[15] N. H. Lipman, "Overview of wind/diesel systems," in *Proc. 1st World Renewable Energy Congr.*, vol. 3, Reading, U.K., 1990, pp. 1547–1563.

[16] T. Ekelund, "Modeling and Linear Quadratic Optimal Control of Wind Turbines," Ph.D. dissertation, Chalmers Univ., Göteborg, Sweden.

[17] E. Welfonder, R. Neifer, and M. Spanner, "Development and experimental identification of dynamic models for wind turbines," *Contr. Eng. Practice*, vol. 5, no. 1, pp. 63–73, 1997.

[18] I. Van de Hoven, "Power spectrum of horizontal wind speed in frequency range from 0.0007 to 900 cycles per hour," *J. Meteorology*, vol. 14, pp. 160–164, 1957.

[19] R. I. Damper, *Introduction to Discrete-Time Signal and Systems*. London, U.K.: Chapman and Hall, 1995, ch. 8, pp. 238–240.

[20] A. M. A. Rodriguez and N. C. Veganzones, "Simulation model for fixed pitch wind turbine with wound rotor induction generators," in *Proc. 1st WREC'92 Conf.*, vol. 3, 1992, pp. 1606–1612.

Cristian Nichita received the Dr.Eng. degree from Dunarea de Jos University, Galati, Romania and the Ph.D. degree from The University of Le Havre, France, in 1995.

He was a member of the Power Electronic Laboratory (LEPII), Le Havre University, from 1992 to 2000, and then joined the Electrotechnic and Automatic Research Team, Le Havre (GREAH), in 2000. He is presently an Assistant Professor (MdC) of electrical engineering at the University of Le Havre. His research interests include wind energy systems and control of real time simulators.

Dragos Luca received the M.Sc. degree from the University of Le Havre, Le Havre, France, in 1998 where he is currently pursuing the Ph.D. degree at the Electrotechnic and Automatic Research Team, Le Havre (GREAH) laboratory.

His research interests are wind energy systems and control techniques.

Brayima Dakyo received the Dr.Eng. degree from Dakar University, Dakar, Senegal, in 1987 and the Ph.D. and Habilitation degrees from the University of Le Havre, Le Havre, France, in 1988 and 1997, respectively.

He was one of the creators of the Power Electronic Laboratory (LEPII), Le Havre University, France, in 1989. From 1989 to 1999, he was Assistant Professor (MdC), Le Havre University. In 2000, he became Professor of electrical engineering and Director of the recently created (2000) Electrotechnic and Automatic Research Team, Le Havre (GREAH). His current interests include power electronic, converter fed electrical machines, electrical powered systems, wind and solar energy systems, diagnostic.

Emil Ceanga received the M.Sc. and Ph.D. degrees from Bucharest Polytechnic Institute, Bucharest, Romania, in 1961 and 1969, respectively.

He is presently Professor of electrical engineering at Dunarea de Jos University, Galati, Romania, and Director of the University Research Center for Advanced Automatic Control Systems. His research interests include intelligent control techniques and renewable energy systems.